ELSEVIER

Journal of Power Sources 104 (2002) 221–225

JOURNAL OF POWER SOURCES

www.elsevier.com/locate/jpowsour

Nanosized Sn–Cu–B alloy anode prepared by chemical reduction for secondary lithium batteries

D.G. Kim[a], H. Kim[b], H.-J. Sohn[a,*], T. Kang[a]

[a]*School of Materials Science and Engineering, Seoul National University, Seoul 151-742, South Korea*
[b]*Materials and Device Laboratory, Samsung Advanced Institute of Technology, Kyungki-do 449-712, South Korea*

Received 19 June 2001; accepted 3 September 2001

Abstract

Nanosized Sn–Cu–B alloy powder is synthesized by chemical reduction to be used as an alternative anode material for secondary lithium batteries. The alloy powder consists of two phases, i.e. mainly η'-Cu_6Sn_5 and a small amount of ε-Cu_3Sn. The reaction of Cu_6Sn_5 with lithium proceeds in two steps. Lithium is inserted into the Cu_6Sn_5 lattice first as $Li_xCu_6Sn_5$, which is isostructural with Li_2CuSn, followed by alloying with tin, reversibly even after long cycling. The cycle performance of the nanosized Cu_6Sn_5 electrode is significantly enhanced in comparison with that of the same material prepared by sintering or mechanical alloying.

Keywords: Cu_6Sn_5; Chemical reduction; Nanosized material; Alloy anode; Secondary lithium battery

1. Introduction

There is an increasing demand for higher-capacity anode materials for secondary lithium batteries. One of the commercial anode materials, graphite, has only 10% (372 mAh g^{-1}) of the theoretical capacity of metallic lithium (3860 mAh g^{-1}). Thus, various anode materials have been investigated to overcome the limited capacity of graphite.

Many alloy systems have been studied as anode materials [1,2]. Although the alloys have much higher capacities than that of graphite, they undergo several phase changes during charge and discharge with severe volume expansion and contraction. This limits the cycle-life of the electrode. The performance of alloy electrodes can be improved significantly if the active alloy is finely dispersed with a less active or inactive component in a composite matrix. It is believed that the less active or inactive species provide structural stability to the composite electrode and combats the expansion of finely-dispersed active particles. For example, various intermetallic compounds such as Sn_xFe [3–5] and Mg_2Si [6] show improved reversible cycling behavior compared with pure active material.

The Cu_6Sn_5 intermetallic compound has also been suggested as one of the alternative anode materials. Kepler et al. [7] reported that Cu_6Sn_5 reacts reversibly with lithium to deliver an initial charge capacity of approximately 350 mAh g^{-1}. Based on structural similarity, it was proposed that this reaction could be described as an insertion of lithium into the Cu_6Sn_5 structure reversibly to form Li_x-Cu_6Sn_5 (isostructural with Li_2CuSn). In recent paper, Larcher et al. [8] reported that the reaction of lithium with Cu_6Sn_5 proceeds in two distinct steps. Lithium was inserted into the Cu_6Sn_5 lattice first as $Li_xCu_6Sn_5$, followed by alloying with tin ($Li_{4.4}Sn + Cu$). These Cu_6Sn_5 intermetallic compounds exhibit improved reversible cycling behavior compared with pure Sn, but cycleability is not so good. It has been shown that decreasing the particle size of active material is an effective way to enhance the mechanical performance of electrodes [9–11]. Since absolute dimensional changes are proportional to the particle size, small particles can reduce the mechanical stress within the particles.

In this study, nanosized Cu_6Sn_5 intermetallic compound is synthesized by chemical reduction to enhance the capacity-retention characteristics. The electrochemical characteristics of Cu_6Sn_5 are studied as an alternative anode material for secondary lithium batteries.

2. Experimental

Nanosized Sn–Cu–B alloy powder was synthesized in 0.05 M $SnCl_2{\cdot}2H_2O$ (Aldrich, 98%) and 0.06 M $CuCl_2{\cdot}2H_2O$ (Aldrich, >99%) solution, using 0.5 M $NaBH_4$ (Aldrich, >98%) as a reducing agent in the presence of a complexant,

* Corresponding author. Tel.: +82-2-880-7226; fax: +82-2-885-9671.
E-mail address: hjsohn@snu.ac.kr (H.-J. Sohn).

0378-7753/02/$ – see front matter
PII: S0378-7753(01)00918-1

$C_6H_5Na_3O_7 \cdot 2H_2O$ (Wako, >99%), under constant mechanical stirring. The pH of the $NaBH_4$ solution was adjusted to about 12 with NaOH (Junsei, >99%) to prevent hydrolysis before reaction. After reaction, the precipitates were filtered, washed thoroughly with distilled water, dilute HCl and acetone. The powder was dried for 48 h at 120 °C under vacuum.

The structure of the powder was identified by means of X-ray diffraction (XRD: MacScience Co., MXP 18A-HF). The composition of the powder was analyzed by inductively coupled plasma spectroscopy (ICP: Shimadzu Co., ICPS-1000IV). The morphology and particle size of the powder were investigated with transmission electron microscopy (TEM: Jeol Co., JEM-200CX).

The electrodes were prepared by coating slurries of active material powders (70 wt.%), carbon black (15 wt.%) and polyvinylidine fluoride (PVDF) (15 wt.%) dissolved in *n*-methyl pyrrolidinone on to a Cu foil substrate. Beaker-type test cells were assembled in an argon-filled glove box (Vac. Co.) using Celgard 2400 as a separator, 1 M $LiPF_6$, ethylene carbonate (EC)/diethyl carbonate (DEC) (1:1 v/v) as an electrolyte, and Li foil as a counter electrode. The charge (Li insertion)–discharge (Li removal) experiments were performed galvanostatically within a voltage window of 0.0–1.2 V.

3. Results and discussion

The XRD pattern of Sn–Cu–B alloy powder prepared by chemical reduction shows that the powder consists of two phases, i.e. mainly η'-Cu_6Sn_5 and a small amount of ε-Cu_3Sn (Fig. 1). The data in Table 1 show that the ratio of Cu to Sn is approximately 6–5, and that powder contains a small amount of boron (0.3 wt.%). The effect of boron can be ignored. Cu_6Sn_5 powder has spherical morphology and the particle size is estimated to be 20–40 nm (see Fig. 2).

Table 1
ICP results for Sn–Cu–B alloy powder prepared by chemical reduction[a]

Sn (mole ratio)	Cu (mole ratio)	Sn (wt.%)	Cu (wt.%)	B (wt.%)
4.8	6	59.72	39.98	0.3

[a] Actual composition (mole ratio and wt.%).

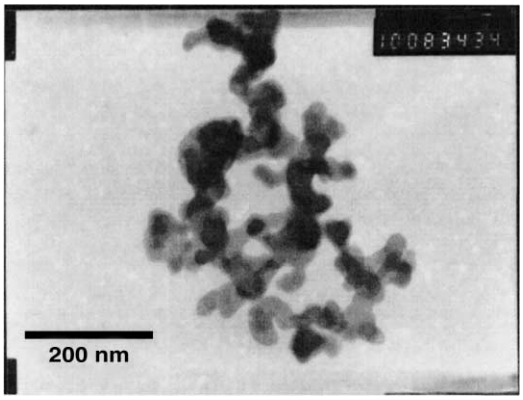

Fig. 2. TEM image of Cu_6Sn_5 powder prepared by chemical reduction.

Voltage profiles for the first charge (Li insertion) and subsequent discharge–charge curves of the Cu_6Sn_5 electrode at a constant current of 200 mA g^{-1} are given in Fig. 3. The theoretical capacity of lithium insertion into Cu_6Sn_5, to form $Li_{13}Cu_6Sn_5$ (isostructural with Li_2CuSn), is 358 mAh g^{-1} for the further alloying reaction of Li with Sn, the maximum lithium insertion capacity is 608 mAh g^{-1} ($Li_{4.4}Sn$). The first charge capacity, 574 mAh g^{-1}, corresponds to a atomic ratio of $Li_{21}Cu_6Sn_5$, which indicates that the Li–Sn alloy phase emerged.

To investigate the electrochemical behavior of Cu_6Sn_5 during Li insertion/removal, differential capacity plots at different currents are compared in Fig. 4. For 30 mA g^{-1} (Fig. 4(a)), two peaks near 400 mV (versus Li/Li^+) and 0 V (versus Li/Li^+) appear during Li insertion, which shows that

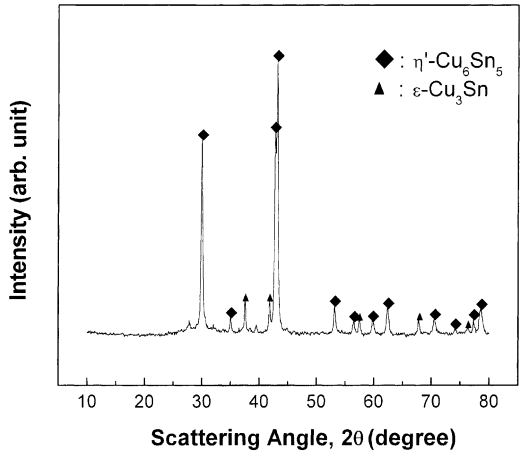

Fig. 1. XRD pattern of Sn–Cu–B alloy powder prepared by chemical reduction.

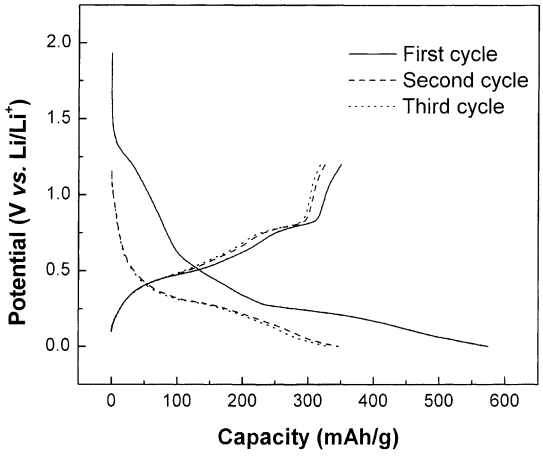

Fig. 3. Voltage profiles for first three cycles of Cu_6Sn_5 electrode.

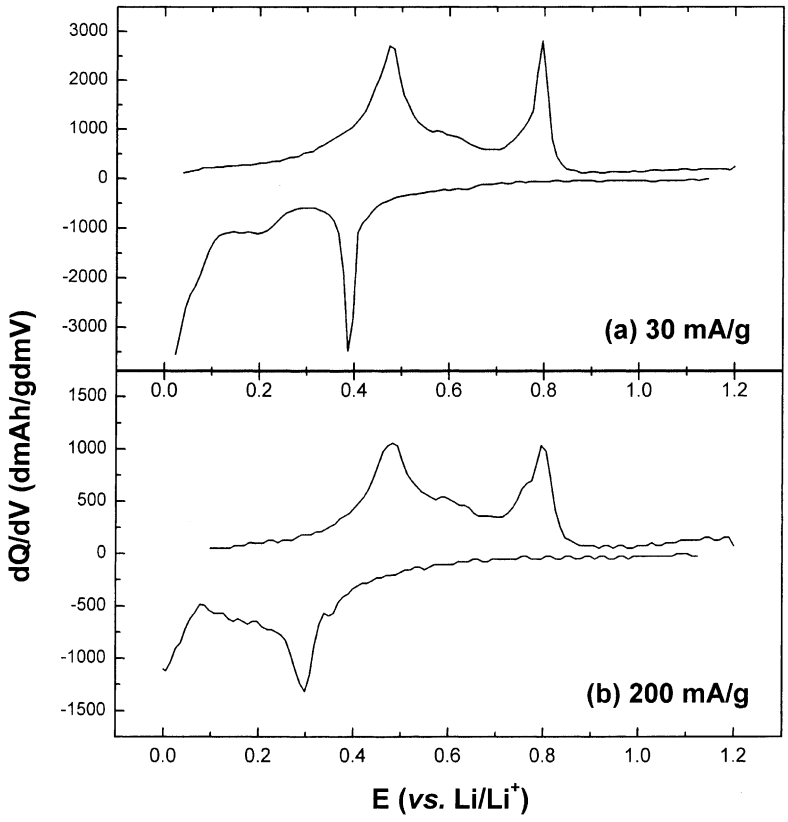

Fig. 4. Differential capacity plots of Cu_6Sn_5 electrodes for first discharge and second charge at different current rates: (a) 30 mA g^{-1}; (b) 200 mA g^{-1}.

Cu_6Sn_5 prepared by chemical reduction follows a similar mechanism to Cu_6Sn_5 prepared by sintering [8]. For 200 mA g^{-1} (Fig. 4(b)), the peak near 400 mV (versus Li/Li^+) shifts to 300 mV (versus Li/Li^+) due to a large overpotential caused by the high rate although the reaction mechanism is not changed. Also fine active material has a short lithium diffusion path and, consequently, the rate capability is enhanced. Since nanosized Cu_6Sn_5 has a good rate capability, which is a very attractive feature as a battery material, all charge–discharge tests were preformed at a constant current of 200 mA g^{-1} in this study.

The XRD patterns of lithiated Cu_6Sn_5 electrodes and electrodes after the removal of lithium are shown in Fig. 5 for various cycles. The data indicate that the reaction proceeds in two steps during charge, which agrees with previous work [8]. Lithium is inserted into the Cu_6Sn_5 lattice first as $Li_xCu_6Sn_5$, which is isostructural with Li_2CuSn and this is followed by alloying with tin as follows [8]:

$$\text{first step}: \quad Cu_6Sn_5 + xLi \Rightarrow Li_xCu_6Sn_5 \quad (\text{isostructural with } Li_2CuSn) \tag{1}$$

$$\text{second step}: \quad Li_2CuSn + (2.4 - x)Li \Rightarrow Li_{4.4-x}Sn + Cu \tag{2}$$

The reverse reactions occur during the discharge process and Cu_6Sn_5 recovers its original crystal structure even after 40 cycles. This behavior is different from other Sn-containing compounds (Sn_2Fe [3], SnSb [11], etc.). In general, a

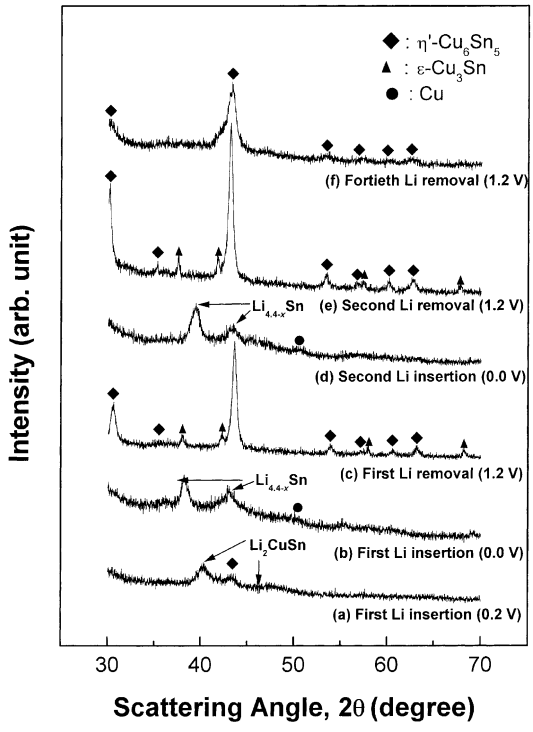

Fig. 5. XRD patterns of Cu_6Sn_5 electrodes after various charge–discharge steps. (a) First Li insertion to 0.2 V (vs. Li/Li^+); (b) first Li insertion to 0.0 V (vs. Li/Li^+); (c) first Li removal to 1.2 V (vs. Li/Li^+); (d) second Li insertion to 0.0 V (vs. Li/Li^+); (e) second Li removal to 1.2 V (vs. Li/Li^+); (f) fortieth Li removal to 1.2 V (vs. Li/Li^+).

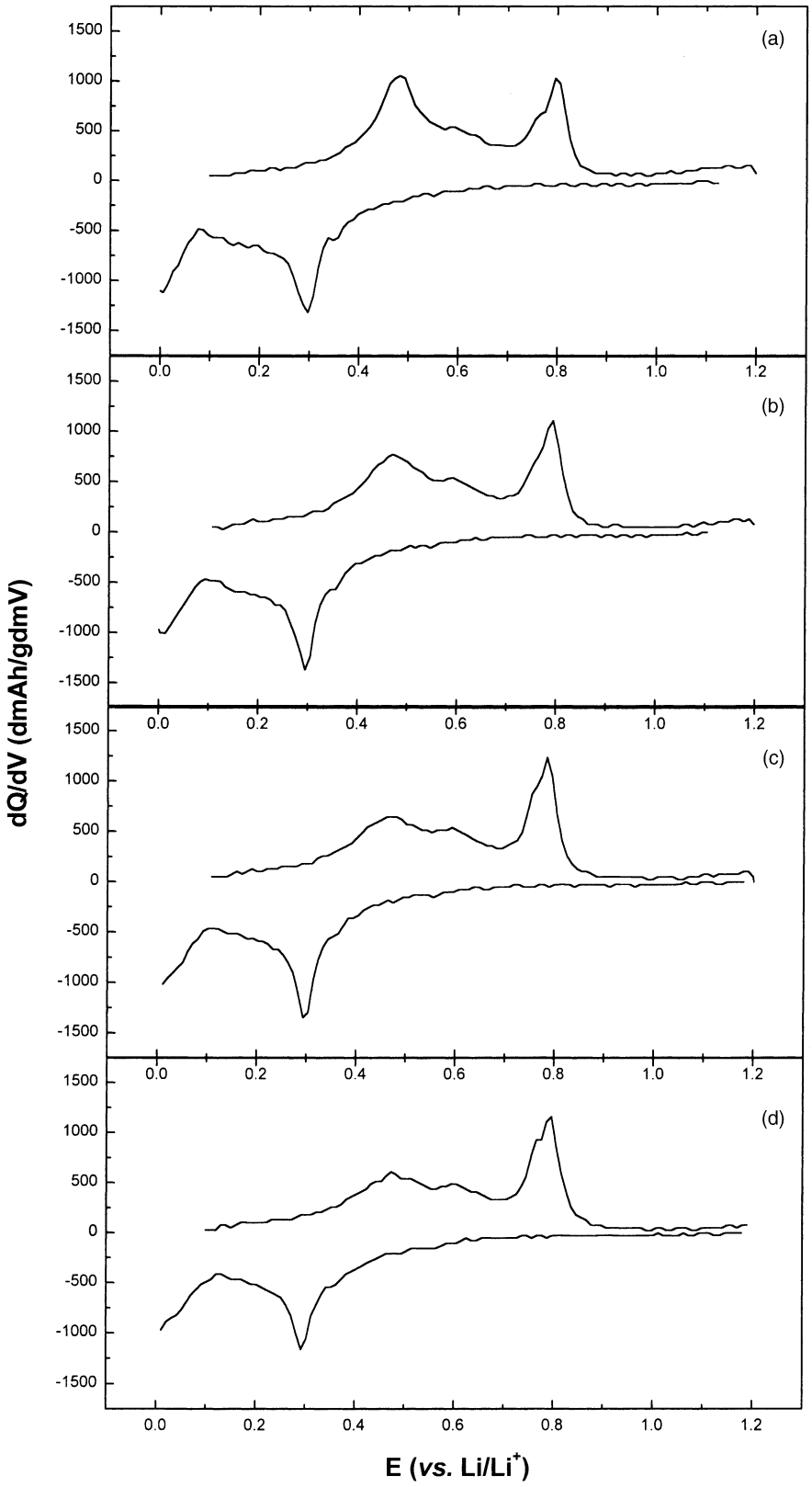

Fig. 6. Differential capacity plots of Cu_6Sn_5 electrode for (a) first; (b) second; (c) 10th; (d) 20th cycle.

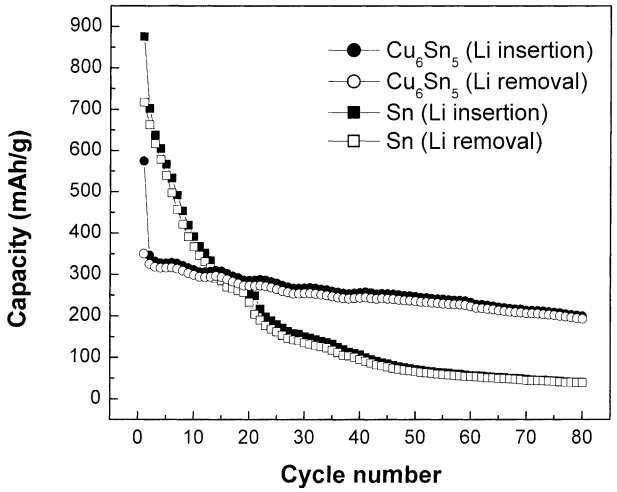

Fig. 7. Capacity vs. cycle number plots for Li/Cu_6Sn_5 and Li/Sn cells for voltage range 0.0–1.2 V (vs. Li/Li^+).

displacement reaction occurs in which the intermetallic structure is broken down to form a series of Li_xM (M:Sn, Sb, etc.) alloys, and then the intermetallic structure is not thoroughly recovered. For these Sn-containing compounds, the original crystal structure collapses and β-Sn is formed within a few cycles. The β-Sn aggregates into large tin region as the cycle number increases. Large tin regions are more sensitive to cracking and crumbling due to higher absolute volume changes than smaller regions. Therefore, it is very beneficial with respect to application as an anode material that Cu_6Sn_5 electrode recovers its original crystal structure and does not show any sign of the formation of β-Sn even after lengthy cycling.

Cu_3Sn phase observed before lithiation disappears after the lithium insertion reaction, and reappears after the lithium removal reaction. This indicates that Cu_3Sn can function as an active material. Differential capacity plots confirm the XRD results (Fig. 6). There is no change in these plots even at 20th cycle. Thus, the reaction mechanism of Cu_6Sn_5 is reversible.

Courtney and Dahn [12] have suggested that reducing the upper cut-off voltage to the 0.8 V hinders the aggregation of the mobile Sn into larger clusters and, thereby, cycle-life was improved. The cycle performance of Li/Cu_6Sn_5 and Li/Sn cells in the voltage range 0.0–1.2 V (versus Li/Li^+) is shown in Fig. 7. The aggregation of Sn into larger clusters has not been observed in this study (Figs. 5 and 6). The cycleability of the Cu_6Sn_5 electrode synthesized by chemical reduction is significantly enhanced compared with that for the same materials when prepared by sintering [7,8] or mechanical alloying [13,14]. This may be mainly caused by two factors: (1) nanosized active material; (2) recovery of the Cu_6Sn_5 intermetallic structure.

As mentioned above, the Cu_6Sn_5 intermetallic compound prepared by chemical reduction recovers its original crystal structure even after extensive cycling. This is an attractive feature as an anode material. Furthermore, the size effect of nanosized active material enhances the cycleability.

4. Conclusions

A nonosized Cu_6Sn_5 intermetallic compound is prepared by chemical reduction in order to enhance the capacity-retention. XRD patterns showed that the Cu_6Sn_5 structure is recovered even after extensive cycling. Differential capacity plots showed that the reaction mechanism of Cu_6Sn_5 is reversible. The cycleability of a Cu_6Sn_5 electrode synthesized by chemical reduction is significantly enhanced in comparison with that of the same material prepared by sintering or mechanical alloying. This improved cycleability may be due to nanosized active material and/or recovery of the Cu_6Sn_5 intermetallic structure even after lengthy cycling. These attractive features suggest that Cu_6Sn_5 is a promising anode material for secondary lithium batteries.

References

[1] J.O. Besenhard, J. Yang, M. Winter, J. Power Sources 68 (1997) 87.
[2] R.A. Huggins, J. Power Sources 81/82 (1999) 13.
[3] O. Mao, R.A. Dunlap, J.R. Dahn, J. Electrochem. Soc. 146 (1999) 405.
[4] O. Mao, J.R. Dahn, J. Electrochem. Soc. 146 (1999) 414.
[5] O. Mao, J.R. Dahn, J. Electrochem. Soc. 146 (1999) 423.
[6] H. Kim, J. Choi, H.-J. Sohn, T. Kang, J. Electrochem. Soc. 146 (1999) 4401.
[7] K.D. Kepler, J.T. Vaughey, M.M. Thackeray, Electrochem. Solid State Lett. 2 (1999) 307.
[8] D. Larcher, L.Y. Besulieu, D.D. MacNeil, J.R. Dahn, J. Electrochem. Soc. 147 (2000) 1658.
[9] J. Yang, M. Wachtler, M. Winter, J.O. Besenhard, Electrochem. Solid State Lett. 2 (1999) 161.
[10] J. Yang, Y. Takeda, N. Imanishi, O. Yamamoto, J. Electrochem. Soc. 146 (1999) 4009.
[11] J. Yang, Y. Takeda, N. Imanishi, J.Y. Xie, O. Yamamoto, Solid State Ionics 133 (2000) 189.
[12] I.A. Courtney, J.R. Dahn, J. Electrochem. Soc. 144 (1997) 2943.
[13] G.X. Wang, L. Sun, D.H. Bradhurst, S.X. Dou, H.K. Liu, J. Alloys Compounds 299 (2000) L12.
[14] Y. Xia, T. Sakai, T. Fujieda, M. Wada, H. Yoshinaga, J. Electrochem. Soc. 148 (2001) A471.